THE JOURNAL OF BIOLOGICAL CHEMISTRY
Vol. 276, No. 24, Issue of June 15, pp. 21070–21076, 2001

Printed in U.S.A.

Structural Compatibility between the Putative Voltage Sensor of Voltage-gated K^+ Channels and the Prokaryotic KcsA Channel*

Received for publication, January 18, 2001, and in revised form, March 21, 2001
Published, JBC Papers in Press, March 26, 2001, DOI 10.1074/jbc.M100487200

Marco Caprini‡§, Stefano Ferroni‡, Rosa Planells-Cases§, Joaquín Rueda¶, Carmela Rapisarda‡, Antonio Ferrer-Montiel§‖, and Mauricio Montal**

*From the ‡Department of Human and General Physiology, University of Bologna, Via San Donato 19/2, 40127 Bologna, Italy, the §Centro de Biología Molecular y Celular and the ¶Departamento de Histología, Universidad Miguel Hernández, 03202 Elche Alicante, Spain, and the **Department of Biology, University of California at San Diego, La Jolla, California 92093*

Sequence similarity among and electrophysiological studies of known potassium channels, along with the three-dimensional structure of the *Streptomyces lividans* K^+ channel (KcsA), support the tenet that voltage-gated K^+ channels (Kv channels) consist of two distinct modules: the "voltage sensor" module comprising the N-terminal portion of the channel up to and including the S4 transmembrane segment and the "pore" module encompassing the C-terminal portion from the S5 transmembrane segment onward. To substantiate this modular design, we investigated whether the pore module of Kv channels may be replaced with the pore module of the prokaryotic KcsA channel. Biochemical and immunocytochemical studies showed that chimeric channels were expressed on the cell surface of *Xenopus* oocytes, demonstrating that they were properly synthesized, glycosylated, folded, assembled, and delivered to the plasma membrane. Unexpectedly, surface-expressed homomeric chimeras did not exhibit detectable voltage-dependent channel activity upon both hyperpolarization and depolarization regardless of the expression system used. Chimeras were, however, strongly dominant-negative when coexpressed with wild-type Kv channels, as evidenced by the complete suppression of wild-type channel activity. Notably, the dominant-negative phenotype correlated well with the formation of stable, glycosylated, nonfunctional, heteromeric channels. Collectively, these findings imply a structural compatibility between the prokaryotic pore module and the eukaryotic voltage sensor domain that leads to the biogenesis of non-responsive channels. Our results lend support to the notion that voltage-dependent channel gating depends on the precise coupling between both protein domains, probably through a localized interaction surface.

Ion channels are multisubunit membrane proteins involved in action potential propagation, neurotransmitter release, and excitation-contraction coupling in excitable tissues. Protein sequence information obtained from recombinant DNA technology has revealed that voltage-gated ion channels form a large superfamily of related proteins that include Na^+, Ca^{2+}, and K^+ channels. Voltage-gated K^+ channels are involved in a host of cellular processes, from setting the resting membrane potential and shaping action potential waveform and frequency to controlling synaptic strength (1). The first K^+ channel cloned from the *Drosophila Shaker* locus (2) seemed to code for a unit similar to one of the four internal repeats of the more complex Na^+ and Ca^{2+} channels, consisting of six α-helical transmembrane segments (S1–S6) and a pore-forming loop (P-loop) (3, 4).

The sequence similarity between voltage-gated K^+ channels and voltage-dependent Na^+ and Ca^{2+} channels suggested a modular architecture of the voltage-gated ion channel family. In this modular context, the N-terminal portion of the eukaryotic voltage-gated proteins up to and including the S4 segment may represent a sensor module, responsible for detecting changes in transmembrane potential (5). This notion appears warranted since work in several laboratories combining mutagenesis and biophysics has demonstrated that perturbation of this domain selectively affects channel gating without altering the permeation properties (6–13). The S5-P-S6 region of voltage-gated channels may represent a "pore" module within the larger protein. Indeed, conduction can be abolished by a pore mutation without affecting channel gating (14).

Examination of the sequence of subsequently cloned potassium channels from diverse sources also substantiates the existence of modularity within the voltage-gated potassium channels (15–17). The genes coding for the inward rectifier class of potassium channels code for a protein analogous to the carboxyl-terminal portion of the voltage-gated potassium channels, the S5-P-S6 region (18). These genes are sufficient to form potassium-selective pores, but with poor intrinsic voltage sensitivity. Further evidence for the modular organization of the potassium channels was provided by the identification of a class of channels consisting of two pore modules, with (19) or without (20, 21) an attached "sensor" module. More recently, a novel structural class of mammalian potassium channels has been discovered, with four transmembrane segments and two pore regions (TWIK-1, TREK-1, TRAAK, TASK, and TASK-2), and activated by different kind of stimuli such as membrane stretch and modification of pH (22).

The identification of the KcsA channel from *Streptomyces lividans* has shown that this channel has the closest kinship to the S5-P-S6 region of the Kv channel family. Moreover, KcsA is most distantly related to eukaryotic inwardly rectifying channels with two putative predicted transmembrane segments (23). Single-channel recording, flux measurements, and ligand binding as-

* This work was supported by grants from the Comisión Interministerial de Ciencia y Tecnología and European Commission Fondos Europeos Desarrollo Regional grant 1FD97-0662-C02-01, and La Fundació la Caixa grant 98/027-00 (to A. F.-M.). Research carried out at the University of California was supported by United States Public Health Service Grant GM-49711. The costs of publication of this article were defrayed in part by the payment of page charges. This article must therefore be hereby marked "*advertisement*" in accordance with 18 U.S.C. Section 1734 solely to indicate this fact.

‖ To whom correspondence should be addressed: Centro de Biología Molecular y Celular, Universidad Miguel Hernández, Avda Ferrocarril s/n, 03202 Elche Alicante, Spain. Tel.: 34-96-665-8727; Fax: 34-96-665-8758; E-mail: aferrer@umh.es.

says have shown KcsA to be a high-conductance, tetrameric, K^+-selective channel with an externally located receptor site for charybdotoxin family peptides (24–26). In addition, the recent crystallization of the KcsA protein has provided a structure for such a pore module, enlightening our knowledge of the molecular basis of ion permeation (27). The sequence similarity between KcsA and Kv channels has led to the notion that the prokaryotic channel may be the bacterial ancestor of the pore module present in eukaryotic channels (23).

Thus, it appears reasonable that voltage-gated potassium channels are structurally modular. It has been recently demonstrated, in channel proteins consisting of the sensor module from mouse Kv1.1 (mKv1.1)[1] and the pore module from fly *Shaker* with inactivation ball removed channel (Shaker), and vice versa, that these putative modules can operate outside their native context (28). To further substantiate the modular design of the Kv channel family, we examined whether it would be feasible to confer voltage sensitivity to the voltage-insensitive prokaryotic ancestor KcsA channel by linking its pore domain to the voltage sensor of eukaryotic Kv channels. Thus, we constructed chimeric channels by replacing the pore domain of mKv1.1 and Shaker with the pore module of the KcsA channel (23). Chimeric Kv channels appear to proceed via appropriate biogenesis pathways, as evidenced by their normal translation, glycosylation, folding, and delivery to the plasma membrane of the injected oocytes. Heterologously expressed chimeras did not show detectable voltage-gated ionic current, although they behaved as strong dominant-negative subunits, completely inhibiting the channel activity of wild-type mKv1.1 and Shaker channels. Taken together, these results lend support to the notion of structural compatibility of both protein domains. Our findings also suggest a higher degree of molecular adaptability for functional coupling of both protein modules.

MATERIALS AND METHODS

Molecular Biology of Chimeric Design

Standard molecular biological techniques were as described (29). Shaker (30) was a gift of L. Toro (UCLA), and KcsA was from S. Choe (Salk Institute). Three versions of KcsA-containing chimeras were designed, and a hemagglutinin (HA) peptide tag was included at the carboxyl-terminal end of mKv1.1 and all chimeric coding regions for immunodetection of the expressed protein.

The mKv1.1(S1–S4,5)-KcsA chimera was constructed by replacing the region of mKv1.1 encompassing the S5 segment to the C-terminal end (amino acids 321–481) with the corresponding residues of KcsA (amino acids 27–160). Polymerase chain reaction was used to introduce a silent *Cla*I site in mKv1.1 at amino acids 321 and 322. Two oligonucleotide primers were also used to amplify KcsA from amino acid 27 through the stop codon while simultaneously introducing a *Cla*I site at amino acid 27 and a *Bam*HI at amino acid 160, subsequently used to subclone KcsA into pGEMHE/mKv1.1. Note that this cloning strategy left a 14-amino acid segment from mKv1.1 (amino acids 482–495) at the C-terminal end of KcsA. The mKv1.1(S1–S4)-KcsA chimera was constructed by replacing the region encompassed by the S4–S5 loop up to the C-terminal end of mKv1.1 (amino acids 311–481) with the complete *KCSA* gene. Polymerase chain reaction was used to introduce a silent *Pst*I site in mKv1.1 at amino acids 311 and 312. KcsA was amplified by polymerase chain reaction, inserting *Pst*I and *Bam*HI sites at amino acids 1 and 160, respectively. The amplified fragment was then subcloned into a silent *Pst*I site and the *Bam*HI site into pGEMHE/mKv1.1. The Shaker(S1–S4,5)-KcsA chimera was constructed by replacing the region of Shaker from amino acid 351 onward with KcsA. A silent *Cla*I site was introduced in Shaker at amino acids 350 and 351. A fragment of KcsA from the first chimera cut at the *Cla*I and *Eco*RV sites 3′ of the stop codon was subcloned into pBluescript/Shaker between the *Cla*I site and a blunted *Xho*I site 3′ of the stop codon. The sequences of the transferred segments were verified by both restriction analysis and dideoxy sequencing (31). For *in vitro* transcription, chimeric and wild-type channel clones were linearized and used as templates with the mMESSAGE mMACHINE kit (Ambion Inc., Austin, TX). For expression in COS-7 mammalian cells, mKv1.1(S1–S4,5)-KcsA, Shaker(S1–S4,5)-KcsA, and wild-type mKv1.1 were subcloned into the mammalian expression vector pCIneo (Promega). Enhanced green fluorescent protein (GFP; gift of R. Tsien, University of California, San Diego) was also subcloned into pCIneo.

Cell Culture Methodology

COS-7 cells (gift of M. Canossa, University of Bologna) were cultured as described (32). The day prior to transfection, COS-7 cells were replated in 35-mm Petri dishes at a density of $2–5 \times 10^4$ cells/dish and maintained in supplemented Dulbecco's modified Eagle's medium. COS-7 cells were transfected with the constructs and GFP by the DEAE-dextran method and assayed for electrophysiological measurements 48–72 h post-transfection (33).

Protein Immunoprecipitation and Immunoblotting

Protein analysis for the different clones was carried out by Western immunoblotting. Oocytes (8–10/sample) were collected and lysed as described (34).

Soluble materials from homogenized oocytes were separated on an SDS-polyacrylamide gel and transferred to a nitrocellulose membrane. The nitrocellulose was blocked and probed with 4 μg/μl anti-HA monoclonal antibody (mAb) (Roche Molecular Biochemicals, Mannheim, Germany), anti-Shaker polyclonal antibody (gift of F. Tejedor, Consejo Superior de Investigaciones Científicas, Universidad Miguel Hernández), or anti-mKv1.1 antibody (Alomone), and proteins were detected with an alkaline phosphatase-conjugated antibody (Sigma). The bands were later visualized using the alkaline phosphatase conjugate substrate kit (Bio-Rad). Immunoprecipitation was carried out with an anti-HA monoclonal antibody (2.5 μg/ml) as described (35). Samples were then boiled in SDS-polyacrylamide gel electrophoresis loading buffer and electrophoresed as described above.

Immunocytochemical Labeling of Channel Protein

Xenopus oocytes injected with transcripts of mKv1.1-HA or HA-tagged chimeras or water were selected 48 and 72 h post-injection, embedded in optimal cutting temperature resin (ProSciTech, Thuringowa, Australia), and quickly frozen. 12-μm-thick sections were cut and fixed in 2% formaldehyde in phosphate-buffered saline for 1 h at room temperature. Immunocytochemical labeling was carried out using an indirect alkaline phosphatase method. After blocking overnight 4 °C in phosphate-buffered saline containing 2% bovine serum albumin and 0.2% Triton X-100, sections were incubated with 2.5 μg/μl anti-HA mAb for 90 min at room temperature. After washing in phosphate-buffered saline, sections were incubated for 90 min at room with an alkaline phosphatase-conjugated anti-mouse secondary antibody (diluted 1:2000; Roche Molecular Biochemicals) in phosphate-buffered saline. The reaction was detected using the Bio-Rad alkaline phosphatase kit. The coverslips were mounted in Eukitt (O. Kindler GmbH & Co., Freiburg, Germany), analyzed, and photographed using a Leica DMRB microscope.

Electrophysiological Recordings

Xenopus Oocytes—In vitro transcribed RNA was injected into *Xenopus* oocytes (~10 ng/oocyte) as described (36). Ionic currents were recorded 2–4 days after injection using a two-electrode voltage clamp (TEC 10CD, NPI Electronic, Tamm, Germany) and PULSE Version 8.09 acquisition software (Heka Electronic, Lambrecht, Germany). The oocytes were continually perfused in barium-containing Ringer's solution (3.8 mM K^+, 114.2 mM Na^+, 2 mM Ba^{2+}, and 10 mM TES, pH 7.4). Electrodes were pulled from Corning 7052 glass (Garner Glass, Claremont, CA) on a P-97 puller (Sutter Instrument Co., Novato, CA). Electrodes were filled with 1 M KCl buffered with 10 mM TES and typically had a resistance of <500 kilo-ohms. The currents were sampled at 4–5 kHz after filtering at 1 kHz. Leak subtraction was accomplished with two inverted quarter amplitude prepulses that were scaled and subtracted from the test pulse. All recordings were made at room temperature (~21 °C).

COS-7 Cells—Membrane currents were recorded in the whole-cell configuration as described in detail (37). Patch pipettes were made from borosilicate glass capillaries (Clark Electromedical, Pangbourne, United Kingdom) using a horizontal puller (P-87, Sutter Instrument Co.) and heat-polished (MF-83, Narishige, Tokyo, Japan) to have a resistance of 2–4 megaohms when filled with the standard internal

[1] The abbreviations used are: mKv1.1, mouse Kv1.1; HA, hemagglutinin; GFP, green fluorescent protein; mAb, monoclonal antibody; TES, 2-{[2-hydroxy-1,1-bis(hydroxymethyl)ethyl]amino}ethanesulfonic acid.

solution (144 mM KCl, 2 mM $MgCl_2$, 10 mM TES, and 5 mM EGTA, buffered with KOH to pH 7.2). All experiments were performed with an external solution containing 140 mM NaCl, 4 mM KCl, 2 mM $CaCl_2$, 2 mM $MgCl_2$, 10 mM TES, and 5 mM glucose, buffered with NaOH to pH 7.4. Voltage stimulation and current recordings were obtained with a patch-clamp amplifier (Jens Meyer, Munich, Germany) interfaced (Labmaster TL-1, Axon Instruments, Inc., Foster City, CA) with a microcomputer equipped with pClamp Version 5.5.1 software (Axon Instruments, Inc.). The currents were low pass-filtered at 3 kHz (−3 dB) and acquired at different sampling rates according to the stimulation protocols. Capacitive transients and series resistance were minimized with the analog circuits of the amplifier. In some experiments, membrane currents were leak-subtracted by using a P/4 protocol (38). An agar bridge electrode, filled with 150 mM NaCl, was used as the reference electrode. All experiments were performed at room temperature (~21 °C).

RESULTS

Design of Chimeric Channels—Given that KcsA exhibits significant sequence similarity to the S5-P-S6 region of Kv channels, it was hypothesized that a chimeric construct consisting of the ancestor KcsA linked to the putative eukaryotic voltage sensor would exhibit voltage-dependent gating properties. For this task, we constructed chimeric channels that combined the S1–S4 domain of mKv1.1 or Shaker and the S5-P-S6 domain of the KcsA channel (Fig. 1, *A–C*, *left panels*). These chimeras are referred to as mKv1.1(S1–S4)-KcsA, mKv1.1(S1–S4,5)-KcsA, and Shaker(S1–S4,5)-KcsA, where S1–S4 denotes the N-terminal domain of the Kv channels up to and including the S4 transmembrane segment and S1–S4,5 additionally incorporates the S4–S5 loop from the eukaryotic channels. We considered the intracellular S4–S5 loop because of its contribution to pore properties (39). The C-terminal end of all chimeras was tagged with a hemagglutinin epitope to facilitate the biochemical and immunological analyses.

Designed Chimeras Do Not Exhibit Voltage-dependent Channel Activity in Xenopus Oocytes or Mammalian Cells—We first assessed whether the designed chimeras exhibit voltage-dependent channel gating. As illustrated in Fig. 1(*A–C*, *right panels*), at variance with wild-type mKv1.1 and Shaker, heterologous expression of the mKv1.1(S1–S4,5)-KcsA, mKv1.1(S1–S4)-KcsA, and Shaker(S1–S4,5)-KcsA chimeras did not elicit voltage-activated outward currents from oocytes held at −80 mV and depolarized from −70 to +100 mV (n = 32). The lack of functional expression was not overcome by larger hyper- or depolarizing steps, by injecting increasing amounts of cRNA, or by co-injecting the α- and β-subunits (data not shown). At variance with homomeric wild-type Shaker-expressing oocytes, chimera-injected cells did not display gating currents (data not shown). The absence of functional expression was not due to lack of protein synthesis, as evidenced by immunodetection of the heterologously expressed chimeras (Fig. 1*E*). The immunoblot displays the presence of two bands with molecular masses of ~60 and ~62 kDa in oocytes injected with mKv1.1(S1–S4,5)-KcsA (Fig. 1*E*, *lanes 2* and *6*) and Shaker(S1–S4,5)-KcsA (*lanes 3* and *7*) chimeras, respectively. mKv1.1-injected oocytes exhibited a band of ~67 kDa (Fig. 1*E*, *lanes 1* and *5*). These proteins were selectively immunopurified with anti-HA mAb (Fig. 1*E*, *lanes 5–7*)

We next addressed the question of whether the heterologous expression system was inadequate for expression of chimeras. cDNAs encoding chimeric channels were then cotransfected in COS-7 cells with GFP to facilitate detection of transfected cells. Fluorescent cells were selected for electrophysiological measurements (Fig. 2*A*). As for oocytes, transfection of chimeras did not result in the expression of voltage-dependent ionic currents in response to either depolarizing steps up to +60 mV or hyperpolarization to −130 mV (n = 23) (Fig. 2, *B* and *C*). In contrast, cells transfected with mKv1.1 or Shaker channels expressed sustained outward currents with kinetic properties overlapping those obtained in oocytes (data not shown).

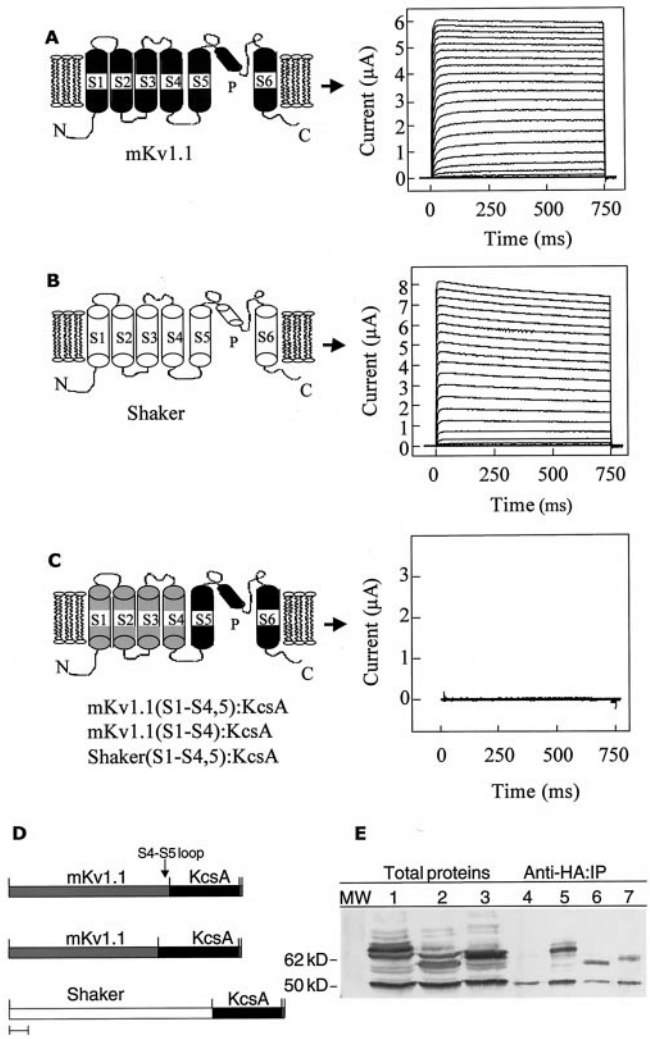

FIG. 1. *A–C*, topological models of mKv1.1, Shaker, and chimeras (*left panels*) and voltage-dependent channel activities of mKv1.1, Shaker, and chimeras (*right panels*), respectively, in *Xenopus* oocytes injected with the corresponding transcripts. Oocytes were held at −80 mV and depolarized up to +100 mV in voltage steps of 10 mV. *D*, molecular design of chimeras containing mKv1.1 and KcsA as voltage sensor and pore module, respectively. In mKv1.1(S1–S4,5)-KcsA, the S4–S5 loop is from mKv1.1, whereas in mKv1.1(S1–S4)-KcsA, it is absent, and KcsA is full-length. Shaker(S1–S4,5)-KcsA is formed by Shaker as voltage module and KcsA as pore module, identical to the mKv1.1(S1–S4,5)-KcsA chimera. The *S4–S5 loop arrow* and the *vertical lines* indicate the approximate location of the chimeric joint. *Scale bar* = 200 base pairs. *E*, immunochemical analysis of protein expression in *Xenopus* oocytes. After cRNA injection in oocytes, proteins were extracted and blotted as total fractions, or immunoprecipitates (*IP*) were generated with the anti-hemagglutinin antibody. Non-injected oocytes were used as a negative control, and mKv1.1-injected oocytes were used as a positive control. *Lane 1–3*, mKv1.1, mKv1.1(S1–S4,5)-KcsA, and Shaker(S1–S4,5)-KcsA total proteins, respectively; *lanes 5–7*, immunoprecipitated fractions. *Lane 4* was non-injected.

Since strong acidification (pH < 5) favors KcsA channel gating (25), we investigated whether extra- and intracellular acidification (pH 4) could promote the appearance of voltage-gated channel activity in chimera-transfected cells. The data indicate that neither extracellular (n = 4) (Fig. 2*D*) nor intracellular (n = 5) (data not shown) acidification evoked channel activity in response to voltage steps. These observations indicate that the linkage of the putative voltage sensor of Kv channels to KcsA does not endow the prokaryotic channel with voltage-dependent channel gating activity.

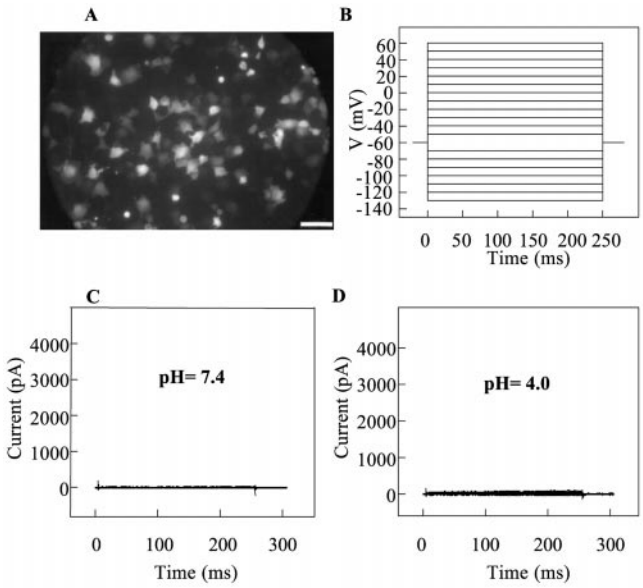

FIG. 2. **Chimeric constructs expressed in COS-7 cells.** *A*, shown is a fluorescence photomicrograph of COS-7 cells cotransfected with GFP and the mKv1.1(S1–S4,5)-KcsA chimera and visualized 72 h post-transfection. *Scale bar* = 60 μm. *B*, a voltage stimulation protocol was employed to activate tight-seal, whole-cell currents in COS-7 cells and consisted of hyperpolarizing and depolarizing steps from −130 to +60 mV in 10-mV increments. The holding potential was −60 mV. *C*, none of the chimeric constructs produced voltage-gated currents. Shown is a representative example of a COS-7 cell transfected with mKv1.1(S1–S4,5)-KcsA at extracellular pH 7.4. *D*, in the same cell, no currents were elicited by lowering the extracellular pH to 4.0 for 2 min.

KcsA-containing Chimeras Exhibit a Dominant-negative Phenotype—To investigate if the translated chimeric subunits have the ability to interact with wild-type channel subunits, we examined whether the chimeras disturbed the channel activity exhibited by wild-type mKv1.1 and Shaker channels in a coexpression experiment. *Xenopus* oocytes were co-injected with both types of subunits, and the channel activity of the presumed heteromeric proteins was compared with that displayed by homomeric proteins. Total cRNA injected was constant in all samples. As illustrated in Fig. 3*A*, oocytes injected with wild-type subunits showed robust voltage-dependent channel activity. By contrast, coexpression of wild-type and chimeric subunits resulted in a virtually complete suppression of wild type-like channel activity. This negative dominance of chimeric subunits was more effective with wild-type mKv1.1 subunits than with wild-type Shaker subunits, as evidenced by the lower amount of chimeric subunit required to inhibit the functional activity of mKv1.1 channels (Fig. 3*A*). The reduction of wild-type channel activity was not due to injection of lower wild-type subunit cRNA amounts since the magnitude of voltage-elicited ionic currents remained fairly invariant as the cRNA injected was decreased from 20 ng (8.2 ± 2.1 μA for mKv1.1 (n = 4) and 12.2 ± 3.0 μA for Shaker (n = 4)) to 5 ng (6.1 ± 1.9 μA for mKv1.1 (n = 4) and 11.2 ± 2.7 μA for Shaker (n = 4)). Therefore, these data indicate a dominant-negative phenotype of the chimeras on wild-type channels.

The occurrence of a dominant-negative phenotype suggests the formation of stable, nonfunctional, heteromeric channels composed of chimeric and wild-type subunits. We used an immunology-based strategy to evaluate this hypothesis. Oocytes co-injected with different molar ratios of wild-type (mKv1.1 or Shaker) and chimeric (mKv1.1(S1–S4,5)-KcsA or Shaker(S1–S4,5)-KcsA) subunits were lysed 72 h post-injection, and chimeric subunits were immunoprecipitated with anti-HA mAb, followed by SDS-polyacrylamide gel electrophoresis. Coprecipitation of mKv1.1 and Shaker subunits was revealed by immunoblotting using either an anti-mKv1.1 antibody raised against the C-terminal domain or an anti-Shaker antibody raised against the N-terminal portion, respectively. As shown in Fig. 3*B* (*upper panel*), immunoblots probed with anti-Kv1.1 mAb revealed a band of >62 kDa corresponding to mKv1.1 in oocytes co-injected with mKv1.1 and mKv1.1(S1–S4,5)-KcsA. A band of ≤62 kDa was also evident as the ratio of mKv1.1(S1–S4,5)-KcsA was increased, indicating that the chimeric channels were also recognized by anti-mKv1.1 antibody, consistent with the presence of a small portion of the epitope in the chimeric subunit (Fig. 1*D*). As expected, these protein bands were absent in mKv1.1-injected and non-injected oocytes. The intensity of the coprecipitated mKv1.1 subunit declined as the amount of mKv1.1(S1–S4,5)-KcsA increased. In contrast, probing the same immunoblots with anti-HA mAb exposed a band of ≤62 kDa only in oocytes injected with mKv1.1(S1–S4,5)-KcsA, which was augmented as the ratio of the chimeric subunit was increased (Fig. 3*B*, *lower panel*). These data are consistent with the formation of stable hetero-oligomers composed of wild-type mKv1.1 and the mKv1.1(S1–S4,5)-KcsA chimera.

Similarly, immunoblots probed with an anti-Shaker antibody raised against the N-terminal domain unmasked the presence of two major bands of ~75 kDa corresponding to Shaker in oocytes injected exclusively with Shaker and Shaker(S1–S4,5)-KcsA subunits and a band of ~62 kDa corresponding to Shaker(S1–S4,5)-KcsA in oocytes containing chimeric subunits (Fig. 3*C*). The intensity of the ~75 kDa band became more faint while that of the ~62 kDa band increased as the amount of chimeric transcripts was augmented in the coexpression system, indicating that the composition of the assembled heteromeric channels is a function of the subunit concentration. The presence of higher molecular mass bands (≥115 kDa) in the immunoprecipitates (Fig. 3*C*), which may correspond to fully *N*-glycosylated subunits in agreement with other reports (40, 41), is also noteworthy. Indeed, treatment of immunoprecipitates with *N*-glycosidase F resulted in the complete and selective disappearance of the higher molecular mass bands for both homomeric Shaker(S1–S4,5)-KcsA and heteromeric Shaker·Shaker(S1–S4,5)-KcsA complexes (Fig. 3*D*). Accordingly, as for mKv1.1-containing chimeras, these findings indicate the formation of stable heteromers between Shaker and Shaker(S1–S4,5)-KcsA subunits. Furthermore, it appears that the heteromeric complexes are *N*-glycosylated, suggesting that they may fold correctly and even be distributed to the plasma membrane.

Homomeric Chimeras Are Delivered to the Plasma Membrane—The dominant-negative strategy suggests that chimeric subunits could assemble as stable oligomers and be delivered to the plasma membrane, where they form nonfunctional channels. However, the retention of these complexes in the endoplasmic reticulum cannot be ruled out. To distinguish between both possibilities, we examined the surface expression of homomeric chimeras in the plasma membrane of *Xenopus* oocytes by immunolabeling microscopy. Injected oocytes were collected 72 h post-injection, and frozen sections were probed by an indirect alkaline phosphatase method using anti-HA primary antibody. As depicted in Fig. 4, whereas non-injected oocytes did not show significant labeling of the plasma membrane, a clear distinct brown ring was evident surrounding wild-type mKv1.1- and chimeric mKv1.1(S1–S4,5)-KcsA- and Shaker(S1–S4,5)-KcsA-injected oocytes. Therefore, this assay indicates that a population of both mKv1.1(S1–S4,5)-KcsA and Shaker(S1–S4,5)-KcsA chimeric oligomers was processed and not retained in the intracellular compartments. Homo-oligomeric proteins assembled in the plasma membrane appear to be nonfunctional channels.

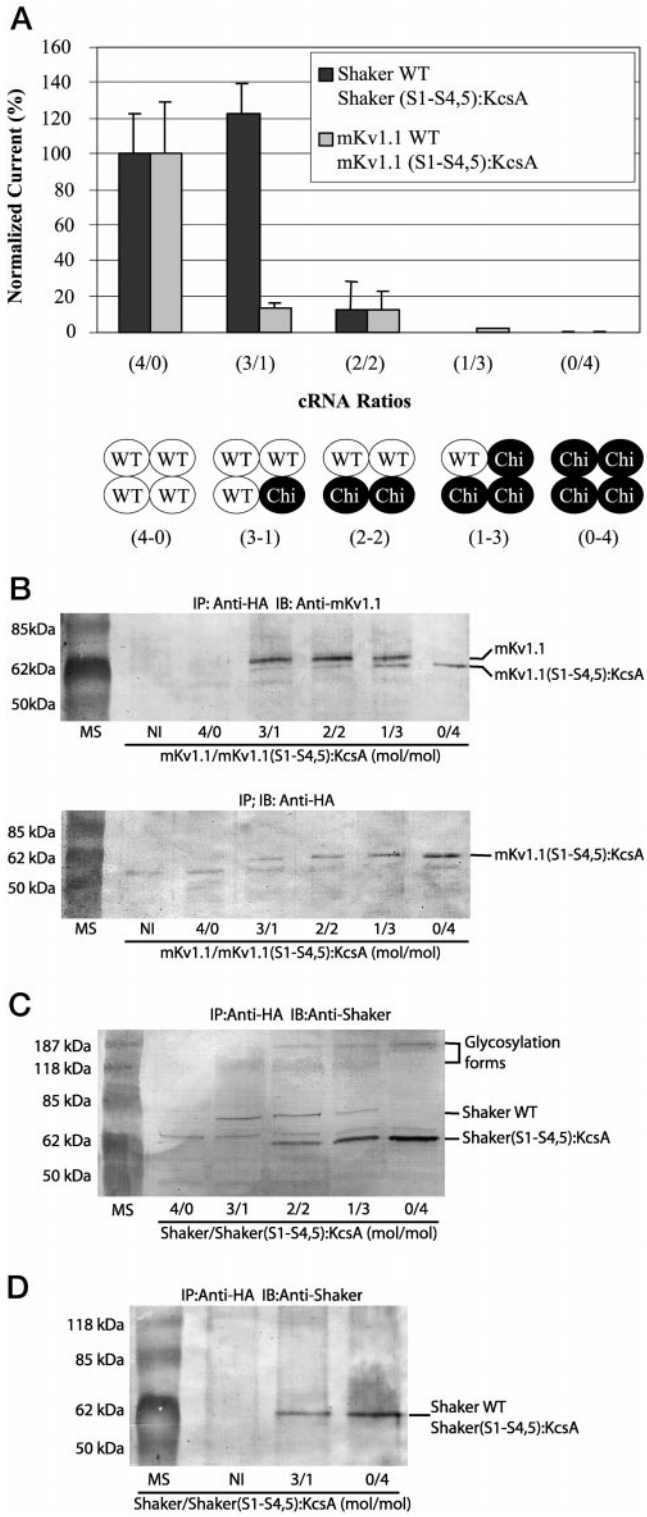

FIG. 3. *A*, chimeric subunits exerted a dominant-negative effect on Shaker and mKv1.1 expression. Wild-type (*WT*) Shaker or mKv1.1 was coexpressed with the indicated chimeric constructs (*Chi*) at 4:0, 3:1, 2:2, 1:3, and 0:4 molar ratios. *Xenopus* oocytes were clamped at −80 mV and depolarized to 0 mV, and current amplitudes were normalized. *B*, wild-type mKv1.1 and mKv1.1(S1–S4,5)-KcsA subunit mRNAs were co-injected in *Xenopus* oocytes, immunoprecipitated, and subjected to immunoblot analysis. The anti-HA epitope antibody was used for immunoprecipitation (*IP*), and the immunoblot (*IB*) was probed with an anti-mKv1.1 antibody raised against a C-terminal peptide sequence present only in the wild-type subunits. The molecular mass standards (*MS*) are shown in the *first lane*. The approximate positions of the protein constructs are indicated on the right. *NI*, Non-injected. *C*, Kv channels and chimeric constructs were coexpressed in *Xenopus* oocytes, immunoprecipitated, and subjected to electrophoresis gel. The anti-HA epitope antibody, present in the C terminus of all chimeric constructs, was used for immunoprecipitation, and the blot was probed with anti-Shaker polyclonal antibody. Both mature (*upper band*) and immature (*lower band*) forms of the Shaker protein are visible, as indicated. *D*, immunoprecipitates obtained from samples generated at 3:1 and 0:4 molar ratios of wild-type Shaker and Shaker(S1–S4,5)-KcsA were subjected to *N*-glycosidase F digestion. The glycosidase hydrolyzed all *N*-glycosidated chains from either the homomeric or heteromeric channels.

DISCUSSION

The remarkable sequence similarity between the prokaryotic KcsA channel and the pore domain of Kv channels suggests that KcsA may be a bacterial ancestor of these eukaryotic channel proteins. Our objective here was to evaluate this model by examining whether KcsA could structurally and functionally replace the pore domain (S5-P-S6) of voltage-gated channels; and additionally, we explored the possibility of endowing the prokaryotic KcsA channel with voltage-dependent gating activity. Replacement of the pore domain of mouse brain (mKv1.1(S1–S4,5)-KcsA) or that of Shaker (Shaker(S1–S4,5)-KcsA) created chimeric channels that failed to express voltage-dependent channel activity or gating currents in *Xenopus* oocytes and a cell line, although they displayed a conspicuous dominant-negative phenotype when coexpressed with wild-type mKv1.1 or Shaker subunits (Fig. 1). The lack of functional expression appeared not to arise from the synthesis of incomplete proteins, as evidenced by the presence of proteins of the expected size in both heterologous expression systems (Fig. 2). A plausible explanation for the nonfunctional phenotype is the retention of chimeric channels in the endoplasmic reticulum because of a misfolding of the subunits that prevents normal trafficking. However, analysis of the pathway of channel biogenesis suggested that chimeras were properly folded and targeted to the cell surface. First, the dominant-negative phenotype exhibited by both chimeric subunits correlates with the formation of stable hetero-oligomers with wild-type subunits (Fig. 3). Second, a significant population of wild-type and chimeric subunits appeared to be heavily glycosylated, presumably at the two glycosylation sites located in the loop connecting the first and second transmembrane segments (40). Although glycosylation is not an essential requirement for the assembly of functional channels at the cell membrane, the presence of two glycosylated forms in the homo- and hetero-oligomer subunits suggests correct folding, assembly, and endoplasmic reticulum/Golgi trafficking of at least a portion of these channel proteins to the plasma membrane. Indeed, immunocytochemical analysis using an anti-HA mAb showed that homo-oligomers of chimeric channel subunits were efficiently expressed on the oocyte plasma membrane, exhibiting a level of expression similar to that of wild-type Kv subunits (Fig. 4). This is significant since the endoplasmic reticulum contains a stringent quality control system that retains misfolded, incomplete, or incorrectly assembled proteins, and only fully assembled channels are transported to the Golgi for further processing and delivery to their functional location (41, 42). Collectively, these findings demonstrate that replacement of the pore module of Kv channel subunits such as mKv1.1 and Shaker with the pore domain of KcsA gives rise to chimeric subunits that fold and assemble into stable complexes that are delivered to the cell surface. Therefore, the prokaryotic pore module represented by KcsA appears to be structurally compatible with the voltage sensor of eukaryotic Kv channels. However, the molecular linkage of two distinct protein modules is not sufficient to express functional coupling between them.

A central question arises: why do chimeric channels fail to display channel activity? The suppression of channel activity

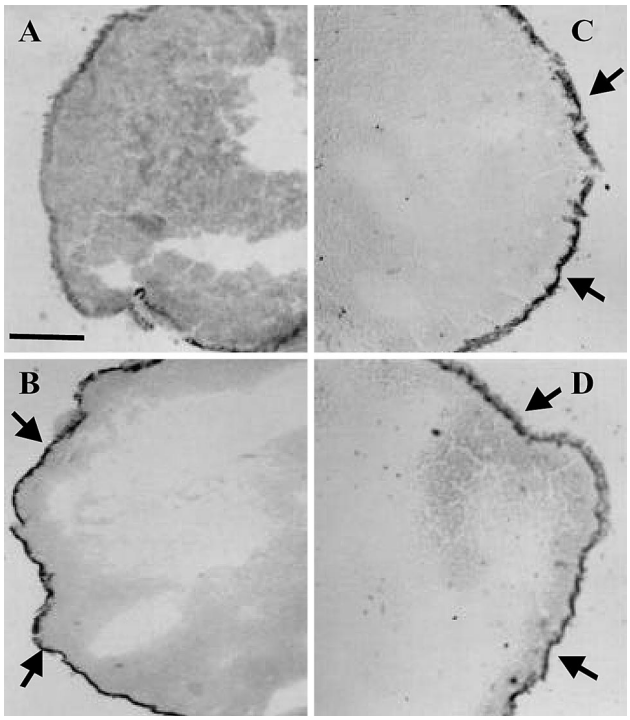

FIG. 4. **Surface expression of wild-type mKv1.1-HA or homomeric chimeras in the plasma membrane of *Xenopus* oocytes detected by immunolabeling microscopy.** Non-injected oocytes did not show significant labeling of the plasma membrane (*A*), whereas a clear distinct brown ring (*arrows*) surrounded wild-type mKv1.1-injected (*B*) and chimeric mKv1.1(S1–S4,5)-KcsA-injected (*C*) and Shaker(S1–S4,5)-KcsA-injected (*D*) oocytes. *Scale bar* = 50 μ m.

by replacement of the pore domain of Kv channels with KcsA implies that the precise coupling interaction between the voltage sensor module and the putative docking site on the pore domain is not effectively restored in the chimeric channels. Presumably, a discrete set of specific and critical protein-protein interaction surfaces between both modules are necessary to couple the movement of the S4 segment to channel opening, but are not essential for correct protein folding. Disruption or perturbation of these interactions would specifically lead to a partial or complete uncoupling of both domains, thus giving rise to the biogenesis of correctly assembled nonfunctional channels (43). In support of this notion, fluorescence scanning studies have led to the identification of protein rearrangements that correlate with voltage-dependent gating and the postulation of the existence of a docking site on the pore domain for accommodating the sensor module (44). Furthermore, a tryptophan scanning strategy has identified an interaction surface for voltage-sensing domains on the pore domain of Shaker near the interface between adjacent pore domain subunits (45). Mutation of residues at the cytoplasmic one-third of the pore results in significant changes in voltage-dependent gating (45). Interestingly, the lowest sequence similarity between the pore modules of Kv channels and KcsA is constrained to the internal domain, where the activation gate may be located (43, 46–49), suggesting a plausible structural divergence in this region. Recent data from blocker protection in the pore of voltage-gated Kv channels are also consistent with the presence of a kink at the level of the highly conserved P*X*P motif present in the S6 helices of Kv channels (50). A kink on the cytoplasmic side of the S6 helix may provide the structural flexibility required to couple voltage sensor movements to the activation gate in Kv channels. This structural relaxation is absent in KcsA because this pore lacks the P*X*P motif in the second transmembrane domain (43, 48, 50). The gating mechanism of KcsA appears to involve rigid body motions of both transmembrane helices (48). Accordingly, it is plausible that KcsA-containing chimeras are not functional because the rigidity of the KcsA pore imposes higher activation energies to couple the voltage-sensing machinery to the channel gate. Should this hypothesis be valid, the reconstitution of the interaction surface of the voltage sensor in the pore domain of KcsA may endow the chimeric channels with voltage-dependent channel activity.

In conclusion, our results indicate that the structural compatibility of the voltage sensor and pore modules produces stable, folded channels, but does not necessarily lead to channel activity. Functional coupling of protein modules appears to depend on a constellation of interactions that probably tune the energetic requirements for efficient voltage gating. Further experimental work is necessary to understand the intricacies underlying coupling of both channel modules.

Acknowledgments—We thank the members of the Ferrer-Montiel laboratory for perceptive comments and helpful suggestions and discussion. We are grateful to Reme Torres for technical assistance with cRNA preparation and oocyte manipulation and injection, Alessia Minardi for technical assistance with cell culturing, and Carolina Garcia-Martinez for comments on the manuscript. We are indebted to L. Toro for the Shaker clone, S. Choe for the KcsA clone, F. Tejedor for the anti-Shaker antibody, M. Canossa for the COS-7 cells, and R. Tsien for the enhanced GFP clone.

REFERENCES

1. Rudy, B. (1988) *Neuroscience* **25,** 729–749
2. Tempel, B., Papazian, D., Schwarz, T., Jan, Y., and Jan, L. (1987) *Science* **237,** 770–775
3. Noda, M., Shimizu, S., Tanabe, T., Takai, T., Kayano, T., Ikeda, T., Takahashi, H., Nakayama, H., Kanaoka, Y., Minamino, N., Kangawa, K., Matsuo, H., Raftery, M. A., Hirose, T., Inayama, S., Hayashida, H., Miyata, T., and Numa, S. (1984) *Nature* **312,** 121–127
4. Tanabe, T., Takeshima, H., Mikami, A., Flokerzi, V., Takahashi, H., Kangawa, K., Kojima, M., Matsuo, H., Hirose, T., and Numa, S. (1987) *Nature* **328,** 313–318
5. Greenblatt, R., Blatt Y., and Montal, M. (1985) *FEBS Lett.* **193,** 125–134
6. Jan, L., and Jan, Y. (1997) *Annu. Rev. Neurosci.* **20,** 91–123
7. Heginbotham, L., Lu, Z., Abramson, T., and MacKinnon, R. (1994) *Biophys. J.* **66,** 1061–1067
8. Papazian, D., Timpe, L., Jan, Y., and Jan, L. (1991) *Nature* **349,** 305–310
9. McCormack, K., Tanouye, M. A., Iverson, L. E., Lin, J. W., Ramaswami, M., McCormack, T., Campanelli, J. T., Mathew, M. K., and Rudy, B. (1991) *Proc. Natl. Acad. Sci. U. S. A.* **88,** 2931–2935
10. Lopez, G. A., Jan, Y., and Jan, L. (1991) *Neuron* **7,** 327–336
11. Perozo, E., Santacruz-Tolosa, L., Stefani, E., Bezanilla, F., and Papazian, D. (1994) *Biophys. J.* **66,** 345–354
12. Planells-Cases, R., Ferrer-Montiel, A., Patten, C., and Montal, M. (1995) *Proc. Natl. Acad. Sci. U. S. A.* **92,** 9422–9426
13. Seoh, S., Sigg, D., Papazian, D. M., and Bezanilla, F. (1996) *Neuron* **16,** 1159–1167
14. Perozo, E., MacKinnon, R., Bezanilla, F., and Stefani, E. (1993) *Neuron* **11,** 353–358
15. Montal, M. (1995) *Annu. Rev. Biophys. Biomol. Struct.* **24,** 31–57
16. Montal, M. (1996) *Curr. Opin. Struct. Biol.* **6,** 499–510
17. Nelson, R., Kuan, G., Saier, M., and Montal, M. (2000) *J. Mol. Microbiol. Biotechnol.* **1,** 281–287
18. Ho, K., Nichols, C., Lederer, W., Lytton, J., Vassilev, P., Kanazirska, V., and Hebert, S. (1993) *Nature* **362,** 31–38
19. Ketchum, K., Joiner, W., Sellers, A., Kaczmarek, L., and Goldstein, S. (1995) *Nature* **376,** 690–695
20. Lesage, F., Guillermare, E., Fink, M., Duprat, F., Lazdunski, M., Romey, G., and Barhanin, J. (1996) *J. Biol. Chem.* **271,** 4183–4187
21. Lesage, F., Guillermare, E., Fink, M., Duprat, F., Lazdunski, M., Romey, G., and Barhanin, J. (1996) *EMBO J.* **18,** 1004–1011
22. Maingret, F., Patel, A. J., Lesage, F., Lazdunski, M., and Honore, E. (1999) *J. Biol. Chem.* **274,** 26691–26696
23. Schrempf, H. Schmidt, O., Kümmerlen, R., Hinnah, S., Müller, D., Betzler, M., Steinkamp, T., and Wagner, R. (1995) *EMBO J.* **14,** 5170–5178
24. Cortes, M., and Perozo, E. (1997) *Biochemistry* **36,** 10343–10352
25. Heginbotham, L., Le Masurier, M., Kolmakova-Partensky, L., and Miller, C. (1999) *J. Gen. Physiol.* **114,** 551–560
26. MacKinnon, R., Cohen S., Kuo, A., Lee, A., and Chait, B. (1998) *Science* **280,** 106–109
27. Doyle, D., Cabral, J., Pfuetzner, R., Kuo, A., Gulbis, J., Cohen, S., Chait, B., and MacKinnon, R. (1998) *Science* **280,** 69–77
28. Patten, C., Caprini, M., Plannells-Cases, R., and Montal, M. (1999) *FEBS Lett.* **17,** 375–381
29. Sambrook, J., Fritsch, E., and Maniatis, T. (1989) *Molecular Cloning: A*

Laboratory Manual, 2nd Ed., Cold Spring Harbor Laboratory, Cold Spring Harbor, NY
30. Stefani, E., Toro, L., Perozo, E., and Bezanilla, F. (1994) *Biophys. J.* **66,** 996–1010
31. Sanger, F., Nicklen, S., and Coulson, A. (1977) *Proc. Natl. Acad. Sci. U. S. A.* **74,** 5463–5467
32. Ferroni, S., Planells-Cases, R., Ahmed, C. M. I., and Montal, M. (1992) *Eur. Biophys. J.* **21,** 185–191
33. Luthman, H., and Magnusson, G. (1983) *Nucleic Acids Res.* **11,** 1295–1308
34. Sun, W., Ferrer-Montiel, A., Schinder, A., McPherson, J., Evans, G., and Montal, M. (1992) *Proc. Natl. Acad. Sci. U. S. A.* **89,** 1443–1447
35. Ferrer-Montiel, A., Canaves, J., DasGupta, B., Wilson, M., and Montal M. (1996) *J. Biol. Chem.* **271,** 18322–18325
36. Ferrer-Montiel, A., and Montal, M. (1994) *Methods Companion Methods Enzymol.* **6,** 60–69
37. Hamill, P., Marty, A., Neher E., Sakmann, B., and Sigworth, F. (1981) *Pfluegers Arch. Eur. J. Physiol.* **391,** 85–100
38. Armstrong, C., and Bezanilla, F. (1977) *J. Gen. Physiol.* **70,** 567–590
39. Slesinger, P., Jan, Y., and Jan, L. (1993) *Neuron* **11,** 739–749
40. Santacruz-Tolosa, L., Huang, Y., Scott, J., and Papazian, D. (1994) *Biochemistry* **33,** 5607–5613
41. Schulteis, C., Nagaya, N., and Papazian, D. (1998) *J. Biol. Chem.* **273,** 26210–26217
42. Zerangue, N., Schwappach, B., Jan, Y., and Jan, Y. (1999) *Neuron* **22,** 537–548
43. Durrel, S., Hao, Y., and Guy, R. (1998) *J. Struct. Biol.* **121,** 263–284
44. Gandhi, C., Loots, E., and Isacoff, E. (2000) *Neuron* **27,** 585–595
45. Li-Smerin, Y., Hackos, D., and Swartz, K. J. (2000) *Neuron* **25,** 411–423
46. Holmgren, M., Shin, K., and Yellen, G. (1998) *Neuron* **2,** 1617–1621
47. Liu, Y., Holmgren, M., Jurman, E., and Yellen, G. (1997) *Neuron* **19,** 175–184
48. Perozo, E., Cortes, D., and Cuello, L. (1999) *Science* **285,** 73–78
49. Tatulian, S., Cortes, M., and Perozo, E. (1998) *FEBS Lett.* **423,** 205–212
50. del Camino, D., Holmgren, M., Liu, Y., and Yellen, G. (2000) *Nature* **403,** 321–325

Structural Compatibility between the Putative Voltage Sensor of Voltage-gated K^+ Channels and the Prokaryotic KcsA Channel

Marco Caprini, Stefano Ferroni, Rosa Planells-Cases, Joaqui?n Rueda, Carmela Rapisarda, Antonio Ferrer-Montiel and Mauricio Montal

J. Biol. Chem. 2001, 276:21070-21076.
doi: 10.1074/jbc.M100487200 originally published online March 26, 2001